Effects of Sequential Proline Substitutions on Amyloid Formation by Human Amylin$_{20-29}$[†]

Daniel F. Moriarty[‡] and Daniel P. Raleigh*[,‡,§]

Department of Chemistry, State University of New York at Stony Brook, Stony Brook, New York 11794-3400, and Graduate Program in Biophysics and Graduate Program in Molecular and Cellular Biology, State University of New York at Stony Brook, Stony Brook, New York 11794

Received July 13, 1998; Revised Manuscript Received October 28, 1998

ABSTRACT: Amylin, also known as islet amyloid polypeptide (IAPP), is the major protein component of the fibril deposits found in the pancreas of individuals with type II diabetes. The central region of amylin, residues 20−29, has been implicated as a key determinate of amyloid formation. To establish which positions are most important for amyloid formation, the wild-type sequence of the 20−29 fragment and a set of 10 variants have been synthesized in which a proline was placed at each position. Proline is energetically unfavorable in the extended cross-β structure found in amyloid. If a particular position is critical for amyloid formation, then substitution with a proline should inhibit amyloid formation. A proline substitution at any position inhibited aggregation and amyloid formation. Substitution of Asn22, Gly24, and residues 26−28 had the largest effect. Fourier transform infrared (FTIR) spectroscopy showed little secondary structure in these peptides, and transmission electron microscopy (TEM) showed mostly amorphous material. The peptides were much more soluble than the wild-type sequence, and no birefringence was observed with Congo Red staining. Proline substitutions at the N (residues 20 and 21) and C termini showed the least effect. These peptides showed the classic fibril morphology, a significant amount of β-sheet structure, and exhibited green birefringence when stained with Congo Red. The results indicate that residues 22, 24, and 26−28 play a key role in formation of amyloid by amylin. Positions 23 and 25 also appear to be important, but may be less critical than positions 22, 24, and 26−28.

Amyloid formation is known to occur in more than 15 different diseases (*1*), including type II diabetes (*2*, *3*) and Alzheimer's disease (*4*). The amyloid deposits formed in all of these diseases have a protein or peptide as their main component, but the exact composition of the deposits varies from disease to disease. Type II diabetes, or non-insulin-dependent diabetes mellitus (NIDDM[1]), is characterized by abnormal β-cell function and increased peripheral insulin resistance. Almost all individuals with NIDDM are found to have amyloid deposits in and around the islets of Langerhans (*5*). The main protein component of these aggregates is islet amyloid polypeptide (IAPP), also known as amylin (*3*, *6*). Amylin is a 37-residue peptide first isolated from amyloid deposits of patients with NIDDM (*6*, *7*). It is synthesized in the β-cells of the pancreas and cosecreted with insulin (*8*−*10*). The mechanism by which the normally soluble amylin is converted into an insoluble aggregate is at present unknown.

Sequence comparison with calcitonin gene-related peptide (CGRP), a homologous peptide which is thought not to form amyloid, has led to the hypothesis that the region corresponding to residues 20−29 is responsible for the amyloidogenic properties of amylin (Figure 1A). A peptide corresponding to the 20−29 fragment of human amylin has been shown to be capable of forming amyloid fibrils. The fibrils appear to be very similar to those formed by the full-length peptide in vitro (*11*), although there is some evidence that the fibrils formed by the shorter peptide may be less stable than those formed by full-length amylin (*12*). Isotope-edited FTIR experiments on amyloid fibrils composed of residues 20−29 of human amylin suggest that residues 24−27 form an antiparallel β-sheet (*13*). Comparison of the primary sequence of amylin derived from different species also highlights the importance of the region of residues 20−29. Rat amylin does not form islet amyloid. Human and rat amylin differ at only six positions, and five of the changes occur between residues 20 and 29 (*14*). Three of these five replacements involve a proline, a residue which is expected to disrupt the ordered structure found in amyloid. β-Sheet

[†] This work was supported by grants to D.P.R. from The American Heart Association-New York State Affiliate, The Pew Charitable Trust, and the New York State Center for Biotechnology. D.P.R. is a Pew scholar in the Biomedical Sciences. D.F.M. was supported in part by a GAANN fellowship from the Department of Education.

* To whom correspondence should be addressed. E-mail: draleigh@ccmail.sunysb.edu.

[‡] Department of Chemistry, State University of New York at Stony Brook.

[§] Graduate Program in Biophysics and Graduate Program in Molecular and Cellular Biology, State University of New York at Stony Brook.

[1] Abbreviations: CD, circular dichroism; CGRP, calcitonin gene-related peptide; DMF, *N*,*N*-dimethylformamide; FMOC, 9-flourenylmethyloxycarbonyl; FTIR, Fourier transform infrared; HCl, hydrochloric acid; HPLC, high-pressure liquid chromatography; IAPP, islet amyloid polypeptide; MALDI, matrix-assisted laser desorption ionization; NIDDM, non-insulin-dependent diabetes mellitus; PAL linker, 5-(4′-Fmoc-aminomethyl-3′,5′-dimethoxyphenoxy)valeric acid; TBTU, 2-(1*H*-benzotriazol-1-yl)-1,1,3,3-tetramethyluronium tetrafluoroborate; TEM, transmission electron microscopy; TFA, trifluoroacetic acid.

10.1021/bi981658g CCC: $18.00
Published on Web 01/20/1999

A

Sequence of Human Amylin

```
1         10          20          30
KCNTATCAT  QRLANFLVHS  SNNFGAILSS  TNVGSNTY
```

B

Peptide	Sequence (20–29)
Wildtype	SNNFGAILSS
S20P	PNNFGAILSS
N21P	SPNFGAILSS
N22P	SNPFGAILSS
F23P	SNNPGAILSS
G24P	SNNFPAILSS
A25P	SNNFGPILSS
I26P	SNNFGAPLSS
L27P	SNNFGAIPSS
S28P	SNNFGAILPS
S29P	SNNFGAILSP

FIGURE 1: (A) The primary sequence of human amylin. The C terminus is amidated, and a disulfide bond connects Cys2 and Cys7. (B) The primary sequence of residues 20−29 of human amylin and of the 10 proline-containing variants. All peptides have an amidated C terminus and a free N terminus.

stacking and the formation of soluble oligomers have been proposed to play a role in the early stages of amyloid formation by amylin, and the presence of multiple prolines in rat amylin is expected to have a profound effect on this process (*15*). Differences in the conformation of the soluble form(s) of amylin also appear to correlate with differences in aggregation behavior. For example, circular dichroism (CD) studies have demonstrated that there are differences in the conformation of the soluble forms of rat and human amylin, although all of the studies are not in complete agreement on the details on the amount of secondary structure present (*16*−*18*). NMR studies with mixed aqueous fluorinated alcohol cosolvents have also reveled differences in the conformation of the region between residues 20−29 in rat and human amylin in this solvent system (*15*).

Full-length amylin is difficult to synthesize and purify, and the shorter 20−29 fragment is an excellent model system with which to study the effects of sequence variation on amyloid formation. Peptide models have a long history in amyloidosis research, particularly in studies of the β-amyloid peptide (*19*−*24*). To study the importance of specific residues in amylin, we have prepared a set of 11 peptides derived from the 20−29 region of amylin. These include the wild-type sequence and 10 variants with a proline at each position. Our experiment relies upon the fact that a proline residue is energetically unfavorable in β-sheet conformations such as the extended cross-β structure (*25*−*27*) found in amyloid. If a particular position is critical for amyloid formation, then substitution with a proline is expected to inhibit amyloid formation. If the position is not crucial, a proline substitution is expected to have little or no effect. A similar approach was used to study a small amyloidogenic fragment of β-amyloid (*28*). Proline residues have also been incorporated into small peptides, termed "β-sheet breaker peptides", which inhibit amyloid formation by β-amyloid (*29*).

Previous work has shown that placing a proline at position 28 of amylin disrupts amyloid formation, whereas a proline at position 25 has some effect and a proline at position 29 had little effect on amyloid formation (*19*). Here we systematically examine the effects of substitution of a proline at each position within the entire 20−29 sequence. This work represents the first comprehensive analysis of every position in the key 20−29 region of amylin. Each of the peptides was tested for its ability to aggregate and form amyloid using a wide range of techniques. In addition to observation of the time required for a peptide solution to form a gel, three other methods were used to test for amyloid formation. Congo Red staining of the gels was used to test for formation of an ordered aggregate. Transmission electron microscopy (TEM) was used to probe the general morphology of any deposits which were formed, and Fourier transform infrared spectroscopy (FTIR) was used to probe the secondary structure of the samples. Taken together, this combination of biophysical techniques allows for a more reliable and complete picture of the effects of a proline substitution on amyloid formation than would be possible using a single method.

Table 1: Expected and Observed Molecular Weights

peptide	expected molecular weight	observed molecular weight
wild-type	1008.1	1007.6
S20P	1018.1	1018.4
N21P	991.1	991.6
N22P	991.1	991.2
F23P	958.0	957.6
G24P	1048.1	1048.1
A25P	1034.1	1034.9
I26P	992.0	991.5
L27P	992.0	992.1
S28P	1018.1	1018.9
S29P	1018.1	1017.7

MATERIALS AND METHODS

Peptide Synthesis and Purification. Peptides were synthesized on a 0.20 mmol scale on a Millipore 9050$^+$ automated peptide synthesizer using standard 9-fluorenylmethoxycarbonyl (Fmoc) chemistry protocols. Use of a resin with a 5-(4′-Fmoc-aminomethyl-3′,5′-dimethoxyphenoxy)valeric acid (PAL) linker afforded C-terminal amidated peptides. Amino acid activation was carried out using 2-(1*H*-benzotriazol-1-yl)-1,1,3,3-tetramethyluronium tetrafluoroborate (TBTU). The first residue to be attached to the resin, all proline residues, all β-branched amino acids, and all residues directly following a β-branched residue were double-coupled. A capping step consisting of a wash with a solution of 5% acetic anhydride and 5% pyridine in DMF was used. The peptide was cleaved from the resin using a solution of 91% TFA, 3% anisole, 3% thioanisole, and 3% ethanedithiol. The crude peptides were purified by reverse phase HPLC using a C-18 preparative column (Vydac). A two-buffer system was utilized with either TFA or HCl as the counterion. Buffer A consisted of H_2O and 0.1% TFA or 0.045% HCl (v/v). Buffer B consisted of 90% CH_3CN and 10% H_2O and either 0.1% TFA or 0.045% HCl (v/v). All peptides were analyzed by matrix-assisted laser desorption ionization (MALDI) TOF MS and amino acid analysis to confirm the identity of the pure products. Mass spectra were recorded using a Bruker Protein TOF MALDI MS system. The mass spectroscopy data are summarized in Table 1.

Sample Preparation and Gel Formation. Samples were prepared using two slightly different methods. One set of

Table 2: Summary of Experimental Results

peptide[a]	time required to observe gel formation[b]	presence of birefringence[c]	position of FTIR band (cm^{-1})	TEM category[d]
wild-type	30 min	yes	1628	type 1
S20P	12 h	yes	1621	type 1
N21P	2 days	yes	1622, 1688	type 1
N22P	#	no*	1645	type 2
F23P	4 days	yes$^+$	1646	type 3
G24P	36 h	no*	1646	types 3 and 2[e]
A25P	3 days	yes	1622, 1689	types 1 and 3[f]
I26P	#	no*	1649	type 2
L27P	#	no*	1648	type 2
S28P	10 days	no*	1649	type 2
S29P	4 days	yes	1626	type 1

[a] Samples were prepared at an apparent concentration of 15 mg/mL in 1% DCl/D_2O as described in Materials and Methods. [b] The samples rapidly became viscous and some formed gels. Gel formation was monitored as described in Materials and Methods. Peptide solutions were examined for aggregation and gel formation every 10 min for 2 h, then every 2 h for 1 day, every 3 h for the next day, and three times a day for the next week. Data were also collected at later time points. # indicates no gel formation after 3 months. [c] * indicates that no birefringence was detected after 3 months using both methods of staining. $^+$ indicates that this peptide stained in the film state but not in the gel state. [d] TEM data were collected between 7 and 9 days after sample preparation. Some samples were also examined after longer time periods. The TEM images are classified as belonging to one of three types. Type 1 images describe aggregates that conform to the general fibril morphology. Type 2 images describe amorphous aggregates only. Type 3 images describe aggregates that have a mixture of classic fibril morphology and amorphous deposits. [e] Samples of the G24P peptide prepared at the higher apparent concentration exhibited type 3 images, while samples prepared at the lower apparent concentration (in 10% acetic acid) gave rise to type 2 images. [f] Type 1 images were observed for samples of the A25P peptide prepared at the higher apparent concentration, while type 3 images were observed from samples prepared at the lower apparent concentration in 10% acetic acid.

samples was prepared by adding 100 μL of 10% acetic acid to 1 mg of peptide. These conditions were chosen to allow comparison with previous studies from other laboratories (*18*, *19*). The samples were vigorously shaken and then incubated at 37 °C. We refer to these samples as prepared at an apparent concentration of 10 mM, but it is important to realize that we do not mean to imply that the peptides are completely soluble. Indeed, the known solubility of the wild-type peptide is considerably lower (*30*). An additional set of samples was prepared by adding 100 μL of 1% DCl/D_2O to 1.5 mg of peptide. These conditions were chosen to facilitate FTIR experiments. The solutions were periodically inspected for gel and/or precipitate formation. Gel formation was monitored by simple ocular inspection and is operationally defined as the time at which the sample had gelled and was unable to flow even when inverted.

Congo Red Staining and Birefringence. A solution of Congo Red (Sigma) was prepared using the method of Puchtler et al. (*31*). Fresh solutions were made before each staining experiment. Sodium chloride was added in excess to an 80% ethanol solution. The solution was vortexed and then filtered. Congo Red was added in excess to the saturated NaCl ethanol solution, and the resulting solution was vortexed and filtered. Ten microliters of the peptide gel was pipetted onto a glass microscope slide, allowed to dry, and then stained for approximately 1 min. Excess Congo Red solution was removed by blotting. All samples were monitored for birefringence using a Nikon SMZ-2T polarizing microscope equipped with a Sony CCD-IRIS camera which was used to display and enhance images.

A second method of staining was developed. Five hundred microliters of the Congo Red solution was placed on a glass slide, and 10 μL of the peptide solution was injected underneath the surface of the Congo Red solution. The sample was monitored for birefringence over a period of several minutes. This method was tested using fibrils formed from insulin with the method of Burke and Rougvie (*32*). Green birefringence was observed using both staining methods.

Transmission Electron Microscopy. A 5 μL sample of the peptide gels or solution was placed on a carbon-coated Foamvar 200 mesh copper grid. The sample was allow to stand for 15−30 s, and then any excess solution was removed by blotting. The samples were negatively stained with 2% (w/v) uranyl acetate and allowed to dry. The samples were then visualized under a JEOL JEM 1200EX transmission electron microscope operating at 80 kEV. The magnification ranged from 12000 to 100000×.

Fourier Transform Infrared Spectroscopy. The peptide samples used for the FTIR experiments were purified by HPLC using HCl as the counterion. Samples in D_2O were placed on CaF_2 plates with a 50 μm Teflon spacer. The peptide solutions were directly examined, or the solvent was evaporated with a gentle stream of nitrogen and the resulting film examined. Spectra were recorded after purging the sample chamber for 15 min. All spectra were recorded on a BioRad FTS-40A FTIR using a DTGS detector with a 2 cm^{-1} resolution. The interferograms from 64 scans were averaged, and the solvent spectrum was subtracted.

RESULTS

Aggregation and Congo Red Staining. Samples of each of the peptides were prepared and tested for gel formation as described in Materials and Methods. Samples prepared in 1% DCl/D_2O were monitored for gel formation and were also used for the Congo Red staining, FTIR, and TEM experiments. These results are summarized in Table 2. It should be noted that the observed times to form a gel are noticeable slower than the reported time to observe significant changes in the turbidity of samples of the wild-type 20−29 peptide (*30*). This is not unreasonable since the results from the two methods describe different processes and the characteristic sharp increase in turbidity that is often observed with studies of amyloidogenic peptides need not correspond to a gel transition. It is also worth noting that gel formation does not necessarily imply formation of amyloid-like material. A proline substitution at any location inhibited aggregation. All of the peptide solutions rapidly became very viscous, and some formed gels. The S20P, N21P, and G24P peptides formed a gel faster than any of the other peptides. Gel formation was relatively rapid for the F23P, A25P, and S29P peptides, while the S28P peptide required a somewhat longer time to form a gel. The N22P, I26P, and L27P peptides showed little sign of gel formation even after several months. All samples were also tested by Congo Red staining. The films derived from the wild-type, S20P, N21P, F23P, A25P, and S29P peptides all displayed the classic green birefringence associated with amyloid formation when stained with

Table 3: Comparison of Congo Red Staining Techniques

peptide[a]	presence of birefringence in film state after Congo Red staining	presence of birefringence in gel state or in the solution state after Congo Red staining
wild-type	yes	yes
S20P	yes	yes
N21P	yes	yes
N22P	no	no
F23P	yes	no
G24P	no	no
A25P	yes	yes
I26P	no	no
L27P	no	no
S28P	no	no
S29P	yes	yes

[a] Samples were prepared at an apparent concentration of 15 mg/mL in 1% DCl/D_2O, stained with Congo Red, and monitored for birefringence as described in Materials and Methods.

Congo Red. In contrast, the films formed by the N22P, G24P, I26P, L27P, and S28P peptides partially dissipated when the Congo Red solution was applied and showed no birefringence. A slight light blue birefringence was detected for the wild-type peptide, and for the S20P, N21P, A25P, and S29P peptides even without Congo Red present, consistent with formation of an ordered array.

Amyloid formation is a concentration-dependent process (*30*, *33*−*37*), and a possible complication is that the process of preparing the films by evaporation of the solvent from the glass slide might promote aggregation. Consequently, a second method of Congo Red staining was developed with which birefringence in the gel or solution state could be monitored. A comparison of the two staining techniques is shown in Table 3. In all but one instance, the F23P peptide, the results from the two methods were the same. In this case, there was no observable birefringence in the gel state after staining with Congo Red, but strong birefringence was observed from samples of the F23P peptide prepared as films. In agreement with the studies of the peptide films, green birefringence was detected for gels of the wild-type peptide and the S20P, N21P, A25P, and S29P peptides. The birefringence observed for the S29P peptide was, however, weaker in the gel state. No birefringence was observed with solutions of the N22P, G24P, I26P, L27P, or S28P peptides. This is also consistent with the results obtained with the peptide films. Addition of either more Congo Red solution or more peptide solution had no effect.

Several of the gel formation time course experiments and several of the Congo Red staining experiments were repeated at lower apparent concentrations (∼10 mM) in 10% acetic acid solutions to facilitate a direct comparison with other published studies (*19*). Westermark and co-workers have previously tested the effect of proline substitutions at positions 25, 28, and 29 using these conditions. Our experiments are consistent with these earlier studies (*19*). In all cases, gel formation and the formation of material which stains heavily with Congo Red were somewhat slower than was observed using the slightly more concentrated samples prepared in D_2O (data not shown). It is important to reiterate that we use the terminology apparent concentration to refer to the concentration that would result if the peptides were completely soluble. Strong birefringence was still observed for the wild-type, S20P, N21P, and S29P

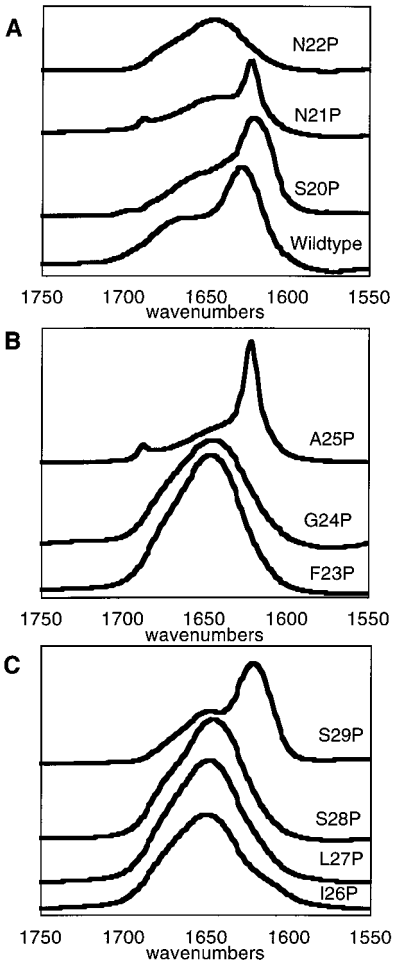

FIGURE 2: FTIR spectra of the peptides derived from the amyloidogenic core of human amylin (residues 20−29). The vertical scale is arbitrary. Spectra are the average of 64 interferograms with a 2 cm^{-1} resolution: (A) wild-type, S20P, N21P, and N22P peptides, (B) F23P, G24P, and A25P peptides, and (C) I26P, L27P, S28P, and S29P peptides.

peptides, and no birefringence was detected for the N22P, G24P, I26P, L27P, or S28P solutions. The only significant discrepancies observed between samples prepared under the two different experimental conditions occurred with the F23P and A25P peptides. For these two peptides, the gels formed from the lower-concentration samples displayed only a slight birefringence even after several months. The results of the gel time course studies and Congo Red staining experiments suggest that amyloid formation is relatively insensitive to a proline substitution at positions 20, 21, and 29. Positions 22, 24, and 26−28 appear to be the most sensitive.

FTIR Studies of Peptide Solutions and Films. FTIR spectra of the peptides were recorded in both the film state and the gel or solution state. The results are summarized in Table 2, and a complete set of spectra are shown in Figure 2. The spectra can be broadly described as belonging to one of two classes, those that are similar to the spectrum of the wild-type peptide and those which resemble the spectrum expected for a disordered peptide. With the exception of that of the A25P peptide, there was little change in the FTIR spectra with longer incubation times. The wild-type peptide and the S20P, N21P, and S29P peptides all showed major peaks between 1621 and 1626 cm^{-1}, diagnostic of β-sheet structure (*38*). Some of the spectra also contained a smaller band at

1688 cm^{-1}, which is thought to be indicative of antiparallel β-structure. As a control, a FTIR spectrum was taken of a sample of the wild-type peptide prepared at an apparent concentration of 15 mM in D_2O which had been incubated for 21 days. Immediately before the spectrum was recorded, the sample was filtered through a PVDF 0.45 μm filter. The intensity of the absorption peak was approximately $^1/_{10}$ of that of the unfiltered solution, and the absorbance peak shifted from 1624 to 1647 cm^{-1}. The filtered solution was stained with Congo Red and showed no birefringence. This indicated that most of the molecules had been converted into an aggregated state that either was larger than 0.45 μm or was sufficiently hydrophobic to stick to the filter surface, while the remaining soluble amylin contained no significant structure. This control experiment demonstrates that the structure which gives rise to the β-sheet FTIR bands is due to aggregated material and not due to soluble fractions of the peptide.

The FTIR spectrum of the N22P, F23P, G24P, I26P, L27P, and S28P peptides all displayed a major absorption band around 1648 cm^{-1}, consistent with these peptides adopting a predominately random conformation. The only peptide which showed time-dependent changes in its FTIR spectra was the A25P peptide. At 10 h, the major absorption peak occurred at 1645 cm^{-1}. After 36 h, the peak shifted to 1622 cm^{-1}. By 48 h, the FTIR spectra gave two distinctive bands at 1621 and 1689 cm^{-1}, indicative of β-structure. No further change was observed. The FTIR experiments show that proline substitution at position 20, 21, or 29 has very little effect on the formation of ordered aggregates. In contrast, a proline substitution at positions 22−24 and 26−28 has a clear effect. These measurements are consistent both with the gel formation studies and with the results of the Congo Red staining experiments.

FTIR measurements were also performed on films of the wild-type, N22P, F23P, G24P, and I26P peptides. In all cases, the bands were much broader, but the spectra of the gel and solution and film states were largely identical with the exception of that of the F23P peptide. The main peak for the F23P peptide was centered around 1635 cm^{-1} with smaller peaks around 1648 and 1655 cm^{-1}, indicating nonrandom structure. This change in structure of F23P from the gel state to the film state is consistent with the Congo Red staining studies.

Electron Microscopy Studies of Aggregates. The peptide samples were viewed by transmission electron microscopy. Clear differences were seen in the micrographs of different peptides, and in some instances within the same sample. TEM was performed on the gel formed from a sample of the wild-type peptide prepared at a nominal concentration of 10 mM and on a gel formed from a sample prepared at a nominal concentration of 15 mM in a 1% DCl/D_2O solution. The 10 mM sample gave rise to fibrils that were 6−10 nm wide and various lengths which appeared morphologically identical to the classic amyloid fibril (Figure 3A). They appeared to be rigid and unbranching, with very few fibrils having a visible twisting repeat. At higher concentrations, there were a combination of 10 and 20−50 nm fibrils, with these wider aggregates appearing to be several narrower fibrils stacked together edge to edge. A similar structure has been observed in fibrils formed from full-length wild-type amylin in vitro (*39*).

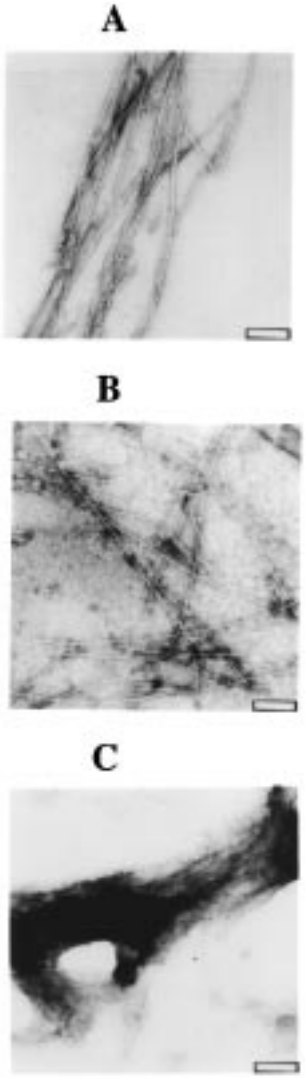

FIGURE 3: TEM micrographs of (A) the wild type (scale bar = 50 nm), (B) N21P peptide (scale bar = 50 nm), and (C) G24P peptide (scale bar = 100 nm).

The fibrils formed by the S20P peptide appeared to be similar to the classic fibril morphology (6−10 nm in width, rigid, and unbranching). Fibrils derived from the N21P peptide were a combination of 6−10 nm, and slightly wider (40−80 nm), fibrils (Figure 3B). The S29P sample produced fibrils which were 6−10 nm wide, matching the classic fibril shape, though a few aggregates contained branching units. These results show that a proline substitution at position 20, 21, or 29 has little effect and are consistent with our other experimental tests of amyloid formation. When the dried samples of the N22P, I26P, L27P, and S28P peptides were visualized, they all were found to be very different from the TEM images of classic amyloid fibrils (Figure 3C). The aggregates were largely unstructured, although a few isolated 10 nm wide fibrils were seen in the L27P peptide sample. These results indicate that substitution of a proline at any of these positions has a major effect upon the ability of the peptide to form amyloid. This observation is entirely consistent with our FTIR, gel formation, and Congo Red staining experiments.

The deposits formed by the F23P, G24P, and A25P peptides differed slightly from the others. The aggregates formed by the F23P peptide showed a combination of classic

fibril morphology, slightly thicker ribbon-like fibrils, and completely unstructured aggregates. The aggregates formed from the more dilute solution (apparent concentration of 10 mM in 10% acetic acid) of the G24P peptide were completely amorphous, while the aggregates formed from the more concentrated solution (apparent concentration of 15 mM) were largely comprised of amorphous material, although a few clusters of fibrils were detected. Over the course of 2 months, no change in structure was observed. The deposits derived from a 10 mM solution of the A25P peptide were unstructured with a few 10 nm wide fibrils. The deposits derived from a 15 mM solution (apparent concentration) of the A25P peptide contained pairs of fibrils which twisted around one another. Twisted fibrils have also been observed in studies of the β-amyloid peptide (*40*). Although there is considerable variation in the type of images observed, some trends are evident. The TEM images can be grouped into three general classes. Type 1 images are considered to follow the classic fibril appearance (6−10 nm wide with various lengths). Type 2 images display no discernible ordered macromolecular structure, and appear to be amorphous. Type 3 images are a combination of the type 1 and type 2 images. Under both concentrations studied, the wild-type peptide and the S20P, N21P, and S29P peptides yielded type 1 images. The N22P, I26P, L27P, and S28P peptides gave rise to type 2 images, while the F23P peptide gave rise to type 3 images. At higher apparent concentrations, the A25P peptide gave rise to type 1 images while the G24P peptide produced type 3 images. At lower apparent concentrations, the A25P peptide generated type 3 images, while the G24P peptide sample displayed type 2 images. The data are summarized in Table 2.

DISCUSSION

Our results demonstrate that positions 20, 21, and 29 are not critical for amyloid formation in our model system. Substitution of a proline at these positions slowed the process of gel formation but did not prevent it. All of these peptides contained a significant amount of β-sheet as determined by FTIR, and all three peptides exhibited the classic green birefringence with Congo Red staining. These variants and the wild-type peptide formed amyloid fibrils as judged by TEM.

In contrast, substitution of a proline at position 22, 24, or at positions 26−28 leads to a drastic and significant effect on amyloid formation. Birefringence was not observed for these peptides, and FTIR studies reveled that the peptides were predominately unstructured. The TEM images reveled mostly amorphous deposits composed of very thin, short material. The one position in the putative amyloidogenic core (residues 24−28) that displayed behavior which differed from the rest was residue 25. This peptide appeared to show time-dependent properties as judged by FTIR. This was the only peptide solution where the FTIR spectrum changed over time. After 10 h, the peptide appeared to be mostly unstructured as judged by FTIR. By 48 h, the peptide had adopted a significant amount of β-sheet structure and birefringence was observed with Congo Red staining. The TEM images reveled the presence of twisted fibrils. At lower apparent concentrations, however, the A25P solution showed aggregates without structure as judged by TEM. Several weeks were required for the low-concentration sample to form a gel, and no observable birefringence was detected when it was stained with Congo Red.

The F23P peptide appeared to exhibit different properties in the film and in the gel state. When this peptide was examined in the gel state, it appeared to be predominately unstructured as judged by FTIR, and gave no signs of birefringence when stained with Congo Red. In contrast, when a film was formed from this gel, FTIR indicated the presence of some β-sheet structure. The film produced from this peptide showed intense birefringence after staining with Congo Red. When the film was viewed under the TEM, clear indications of classic amyloid superstructure were observed. There were also indications of much less ordered aggregates. Taken together, these experiments suggest that this peptide has little structure in the gel state, but the process of removing the solvent allows it to form amyloid-like structure. This observation highlights the importance of sample preparation. By testing this peptide at different concentrations and in different states using a broad range of techniques, we have been able to develop a more complete picture of the role of this position in amyloid formation.

Although the primary sequence of the 20−29 region of amylin is clearly a very important determinate of amyloid formation, it is important to realize that it cannot be the sole determinate. For example, previous work has demonstrated that in vitro amyloid formation by full-length amylin is pH-dependent and that the rate is faster at pH values above the pK_a of histidine 18 (*12*). Our model peptides lack this residue and thus should not be expected to reproduce the pH-dependent behavior observed for the full-length peptide. It is also worth noting that synthetic peptides corresponding to the primary sequence of residues 20−29 of the rabbit and the European hare are amyloidogenic in vitro even though islet amyloid is apparently not observed in these species (*41*). In addition, the sequences of canine (*42*) and feline (*43*) amylin are identical from residue 20 to 29; however, cats form islet amyloid, while dogs do not. Dogs do however form amyloid deposits in insulinomas, and these deposits are comprised of amylin (*44*, *45*). The observation that dogs form amyloid deposits derived from amylin in insulinomas but do not form islet amyloid suggests that factors such as the local concentration of amylin or the conditions in which amylin is secreted, synthesized, and stored play a part in amyloid formation (*44*, *45*). Nonetheless, it is clear that residues 20−29 play a crucial role in amyloid formation and that a certain type of sequence in this region is necessary, but not always sufficient, for amyloid formation.

In this study, we have been able to determine which residues are most important for amyloid formation. We have clearly shown that certain positions play a critical role in determining the amyloid-forming properties of amylin. These results provide a more complete picture of the importance of each residue. Our experimental results demonstrate that a proline substitution at position 20, 21, or 29 has less effect on amyloid formation than a proline substitution at positions 22−28. These observations strongly support models of the amyloid structure which emphasize a more important role for residues in the center rather than at the N or C termini, and they do not support structural models which postulate an important role for position 29 (*13*, *30*, *46*). Previous isotope-edited FTIR and solid state NMR studies of amylin peptides have led to a two-dimensional model of the amyloid

fibril which suggests an important role for positions 24−27 (*13*, *46*). Our work is broadly consistent with these studies, although our data indicate, in agreement with the earlier studies of Westermark and co-workers, that position 28 is also important (*19*). The results of our study also hint, in agreement with previous work, that position 25 is more tolerant of substitutions and hence perhaps less critical than the other core positions (*19*). It is, however, important to reiterate that a proline substitution at position 25 does have noticeable effects on amyloid formation even if they are less pronounced than the effect of substitutions at other positions. There have been somewhat conflicting reports on the importance of this position. The FTIR and solid state NMR studies indicate that it is important, while some earlier studies with synthetic peptides have suggested that position 25 can tolerate a proline mutation (*19*). Our experiments indicate that substitution of residue with a proline does effect aggregation and amyloid formation and in that regard supports the NMR and FTIR studies. Our studies have also clearly shown that position 22 is very sensitive to proline substitution and thus presumably plays a role in the amyloid fibril. This is a very interesting result since previous structural studies have paid little attention to this position. Our experiments indicate that any detailed model of the amyloid structure will need to account for the importance of this residue.

It is striking that single proline substitutions can have such a large effect on the aggregation properties of these peptides. This work suggests a potential strategy for inhibiting aggregation and amyloid formation in bioactive peptides which are of potential therapeutic interest; insertion of a proline at critical locations in amyloidogenic peptides is expected to severely inhibit amyloid formation (*47*, *48*). The ability of proline residues to destabilize β-sheets has also been exploited in the development of small peptides designed to inhibit amyloid formation (*28*, *49*).

ACKNOWLEDGMENT

We thank Professors Fowler and Lauher for the use of their polarizing microscope and Professor Tonge for the use of his FTIR instrument and for numerous helpful discussions. We also thank Brian Kuhlman and Melanie Nilsson for critical review of the manuscript. Electron microscopy studies were carried out with the help of Greg Rudoman at the University Microscopy Imaging Center at the State University of New York at Stony Brook. MALDI MS data were collected at the CASM facility at the State University of New York at Stony Brook.

REFERENCES

1. Sipe, J. D. (1994) *Crit. Rev. Clin. Lab. Sci. 31*, 325−354.
2. Westermark, P., and Wilander, E. (1978) *Diabetologia 15*, 17−21.
3. Clark, A., Cooper, G. J. S., Lewis, C. E., Morris, J. F., Willis, A. C., Reid, K. B. M., and Turner, R. C. (1987) *Lancet 2*, 231−234.
4. Selkoe, D. J. (1991) *Neuron 6*, 487−489.
5. Westermark, P., and Grimelius, L. (1973) *Acta Pathol. Microbiol. Scand., Sect. A 81*, 291−300.
6. Westermark, P., Wernstedt, C., Wilander, E., Hayden, D. W., O'Brien, T. D., and Johnson, K. H. (1987) *Proc. Natl. Acad. Sci. U.S.A. 84*, 3881−3885.
7. Cooper, G. J. S., Willis, A. C., Clark, A., Turner, R. C., Sim, R. B., and Reid, K. B. M. (1987) *Proc. Natl. Acad. Sci. U.S.A. 84*, 8628−8632.
8. Clark, A., Edwards, C. A., Ostle, L. R., Sutton, R., Rothbard, J. B., Morris, J. F., and Thurner, R. C. (1989) *Cell Tissue Res. 257*, 179−185.
9. Cooper, C. J. S. (1994) *Endocr. Rev. 15*, 163−201.
10. Sanke, T., Hanabusa, T., Nakano, Y., Oki, C., Okai, K., Nishimura, S., Kondo, M., and Nanjo, K. (1991) *Diabetologia 34*, 129−132.
11. Glenner, G. G., Eanes, D., and Wiley, C. (1988) *Biochem. Biophys. Res. Commun. 155*, 608−614.
12. Charge, S. B. P., de Koning, E. J. P., and Clark, A. (1995) *Biochemistry 34*, 14588−14593.
13. Ashburn, T. T., Auger, M., and Lansbury, P. T., Jr. (1992) *J. Am. Chem. Soc. 114*, 790−791.
14. Asai, J., Nakazato, M., Kangawa, K., Matsukura, S., and Matsuo, H. (1989) *Biochem. Biophys. Res. Commun. 164*, 400−405.
15. Cort, J., Liu, Z., Lee, G., Harris, S. M., Prickett, K. S., Gaeta, L. S. L., and Andersen, N. H. (1994) *Biochem. Biophys. Res. Commun. 204*, 1088−1095.
16. McLean, L. R., and Balasubramaniam, A. (1992) *Biochim. Biophys. Acta 1122*, 317−320.
17. Hubbard, J. A. M., Martin, S. R., Chaplin, L. C., Bose, C., Kelly, S. M., and Price, N. C. (1991) *Biochem. J. 275*, 785−788.
18. Kapuniotu, A., Bernhagen, J., Greenfield, N., Al-Abed, Y., Teichberg, S., Frank, R. W., Voelter, W., and Bucala, R. (1998) *Eur. J. Biochem. 251*, 208−216.
19. Westermark, P., Engstrom, V., Johnson, K., Westermark, G., and Betsholtz, C. (1990) *Proc. Natl. Acad. Sci. U.S.A. 87*, 5036−5040.
20. Esler, W. P., Stimson, E. R., Ghilardi, J. R., Lu, Y. A., Felix, A. M., Vinters, H. V., Mantyh, P. W., Lee, J. P., and Maggio, J. E. (1996) *Biochemistry 35*, 13914−13921.
21. Halverson, K. J., Sucholeiki, I., Ashburn, T. T., and Lansbury, P. T., Jr. (1991) *J. Am. Chem. Soc. 113*, 6701−6703.
22. Hilbich, C., Kiester-Woike, B., Reed, J., Masters, C. L., and Beyreuther, K. (1992) *J. Mol. Biol. 228*, 460−473.
23. Jarrett, J. T., Costa, P. R., Griffin, R. G., and Lansbury, P. T., Jr. (1994) *J. Am. Chem. Soc. 116*, 9741−9742.
24. Lansbury, P. T., Jr., Costa, P. R., Griffiths, J. M., Simon, E. J., Auger, M., Halverson, K. J., Kocisko, D. A., Hendsch, Z. S., Ashburn, T. T., Spencer, R. G. S., Tidor, B., and Griffin, R. G. (1995) *Nat. Struct. Biol. 2*, 990−998.
25. Minor, D. L., Jr., and Kim, P. S. (1994) *Nature 367*, 660−663.
26. Smith, C. K., Withka, J. M., and Regan, L. (1994) *Biochemistry 33*, 5510−5517.
27. MacAuthur, M. W., and Thornton, J. M. (1991) *J. Mol. Biol. 218*, 397−412.
28. Wood, J. W., Wetzel, R., and Martin, J. D. (1995) *Biochemistry 34*, 724−730.
29. Soto, C., Sigurdsson, E. M., Morelli, L., Kumar, R. A., Castano, E. D., and Frangione, B. (1998) *Nat. Med. 4*, 822−826.
30. Ashburn, T. T., and Lansbury, P. T., Jr. (1993) *J. Am. Chem. Soc. 115*, 11012−11013.
31. Puchtler, H., Sweat, F., and Levine, M. (1962) *J. Histochem. Cytochem. 10*, 355−364.
32. Burke, M. J., and Rougvie, M. A. (1972) *Biochemistry 11*, 2435−2439.
33. Jarrett, J. T., and Lansbury, P. T., Jr. (1993) *Cell 73*, 1055−1058.
34. Jarrett, J. T., and Lansbury, P. T., Jr. (1992) *Biochemistry 31*, 12345−12352.
35. Come, J. H., Fraser, P. E., and Lansbury, P. T., Jr. (1993) *Proc. Natl. Acad. Sci. U.S.A. 90*, 5959−5963.
36. Jarrett, J. T., Berger, E. P., and Lansbury, P. T., Jr. (1993) *Biochemistry 32*, 4693−4697.
37. Esler, W. P., Stimson, E. R., Ghilardi, J. R., Vinters, H. V., Lee, J. P., Mantyh, P. W., and Maggio, J. E. (1996) *Biochemistry 35*, 749−757.

38. Krimm, S., and Bandekar, J. (1986) *Adv. Protein Chem. 38*, 181−364.
39. Goldsbury, C. S., Cooper, G. J. S., Goldie, K. N., Muller, S. A., Saafi, E. L., Gruijters, W. T. M., Misur, M. P., Engel, A., Ueli, A., and Kistler, J. (1997) *J. Struct. Biol. 119*, 17−27.
40. Harper, J. D., Lieber, C. M., and Lansbury, P. T., Jr. (1997) *Chem. Biol. 4*, 951−959.
41. Christmanson, L., Betsholtz, C., Leckstrom, A., Engstrom, U., Cortie, C., Johnson, K. H., Adrian, T. E., and Westermark, P. (1993) *Diabetologia 36*, 183−188.
42. Ohagi, S., Nishi, M., Bell, G. I., Ensinck, J. W., and Steiner, D. F. (1991) *Diabetologia 34*, 555−558.
43. Nishi, M., Chan, S. J., Nagamatsu, S., Bell, G., and Steiner, D. F. (1989) *Proc. Natl. Acad. Sci. U.S.A. 86*, 5738−5742.
44. Jordon, K., Murtaugh, M. P., O'Brien, T. D., Westermark, P., Betsholtz, C., and Johnson, K. H. (1990) *Biochem. Biophys. Res. Commun. 169*, 502−508.
45. O'Brien, T. D., Westermark, P., and Johnson, K. H. (1990) *Vet. Pathol. 27*, 200−204.
46. Griffiths, J. M., Ashburn, T. T., Auger, M., Costa, P. R., Griffin, R. G., and Lansbury, P. T., Jr. (1995) *J. Am. Chem. Soc. 117*, 3539−3546.
47. Brower, V. (1997) *Nat. Biotechnol. 15*, 935−935.
48. Moriarty, D. F., and Raleigh, D. P. (1998) *Biochem. Biophys. Res. Commun. 245*, 344−348.
49. Soto, C., Kindy, M. S., Baumann, M., and Frangione, B. (1996) *Biochem. Biophys. Res. Commun. 226*, 672−680.

BI981658G